Supporting Information

Enhancement of eletrocatalytic abilities toward CO_2 reduction by tethering redox-active metal complexes to the active site.

Habib Md. Ahsan[1,2], Brian K. Breedlove[1,*], Cosquer Goulven[3] Masahiro Yamashita[1,4]

[1]Department of Chemistry, Graduate School of Science, Tohoku University, 6-3 Aza-Aoba, Aramaki, Sendai 980-8578, Japan

[2]Chemistry Discipline, Science, Engineering and Technology School, Khulna University, Khulna-9208, Bangladesh.

[3]Chemistry Department, Graduate School of Science, Hiroshima University, 1-3-1, Kagamiyama, Higashihiroshima, Hiroshima, 739-8526, Japan

[4]School of Materials Science and Engineering, Nankai University, Tiajin 300350, China

Contents and page

1. ^{1}H NMR spectrum of (pic_4cyclen)……3

2. ^{13}C NMR spectrum of (pic_4cyclen)……4

3. ^{1}H NMR spectrum of (bn_4cyclen)……5

4. ^{13}C NMR spectrum of (bn_4cyclen)……6

5. ORTEP diagram of $(pic)_4$cyclen……7

6. Crystal data for $(pic)_4$cyclen……8

7. ESI-Mass of $[([Ru]pic)_4cyclen]^{4+}$……9

8. Crystal data for [bn_4cyclenNiCl]Cl……10

9. Comparison of the coordination geometry of the Ni ion in [bn_4cyclenNiCl]Cl……10

10. The diffusion coefficient calculation……11–12

11. Cyclic voltammograms of $[\{([Ru]pic)_4cyclen\}NiCl]^{5+}$ at different scan rates……11

12. Plot of i_p vs. $v^{1/2}$ for $[\{([Ru]pic)_4cyclen\}NiCl]^{5+}$……12

13. FTIR spectroscopy……13

14. CPE experiment trace……14

15. Cyclic voltammogram of $[Ru(bpy)_2Cl]^+$ ([Ru])……15

16. Cyclic voltammogram of 1:4 [bn_4cyclenNiCl]Cl and $Ru(bpy)_2Cl_2$……16

17. Comparison of CO_2 reduction electrocatalysts……………………………………………………………………17

18. Experimental TOF calculation……………………………………………………………………………………18

19. References………18

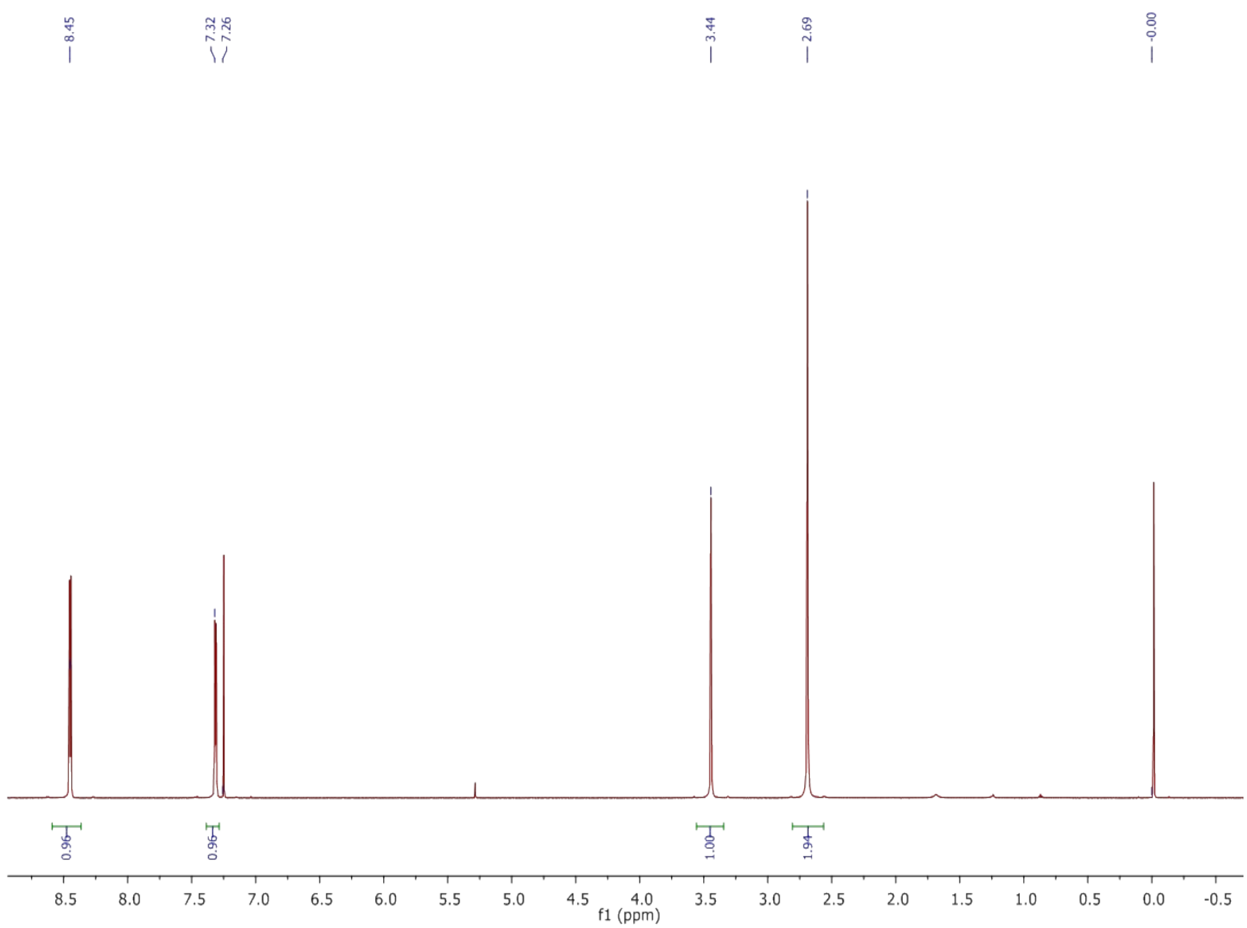

Fig. S1. ^{1}H NMR spectrum of (pic$_4$cyclen)

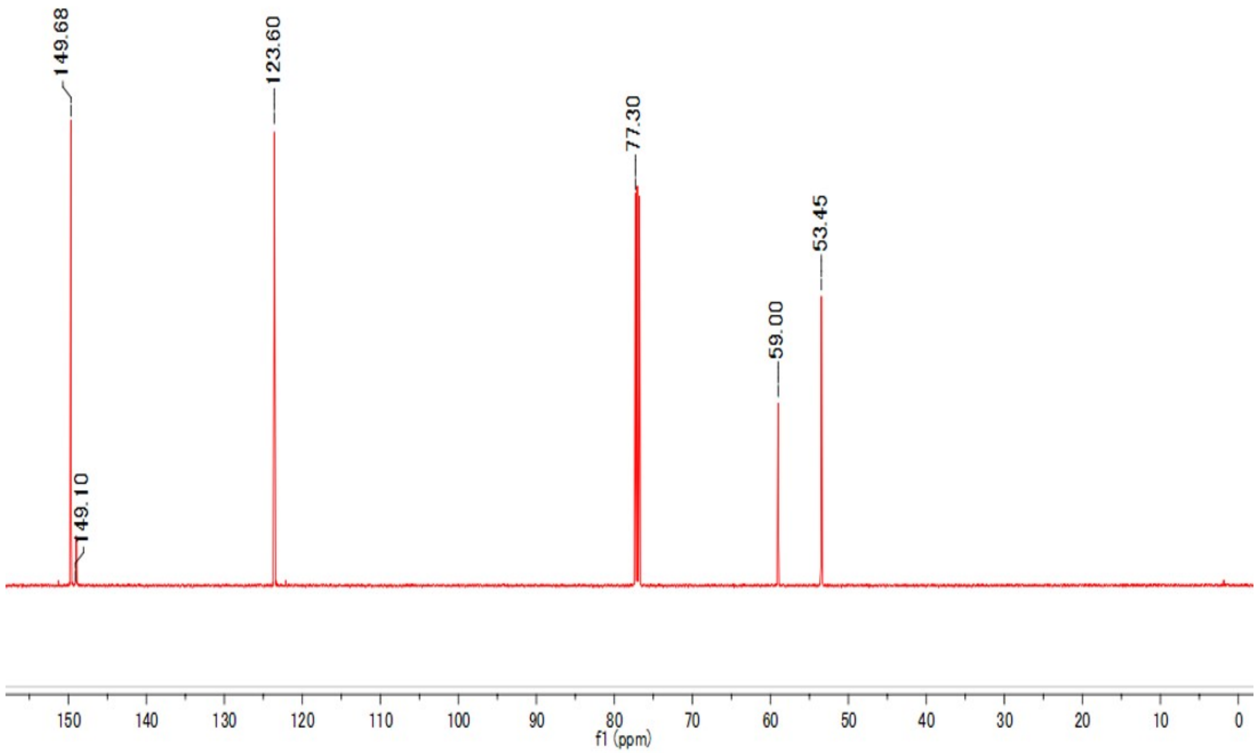

Fig. S2. ^{13}C NMR spectrum of (pic$_4$cyclen)

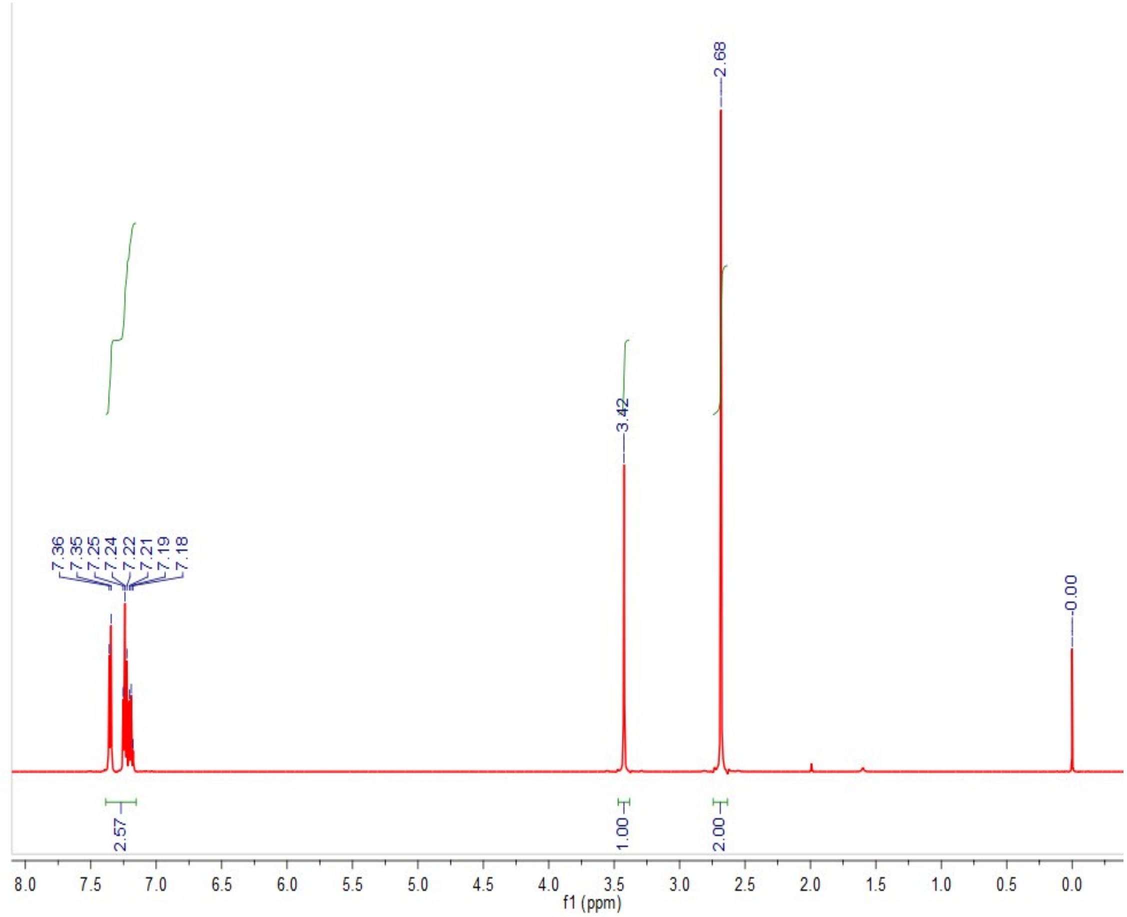

Fig. S3. ^{1}H NMR spectrum of (bn_4cyclen)

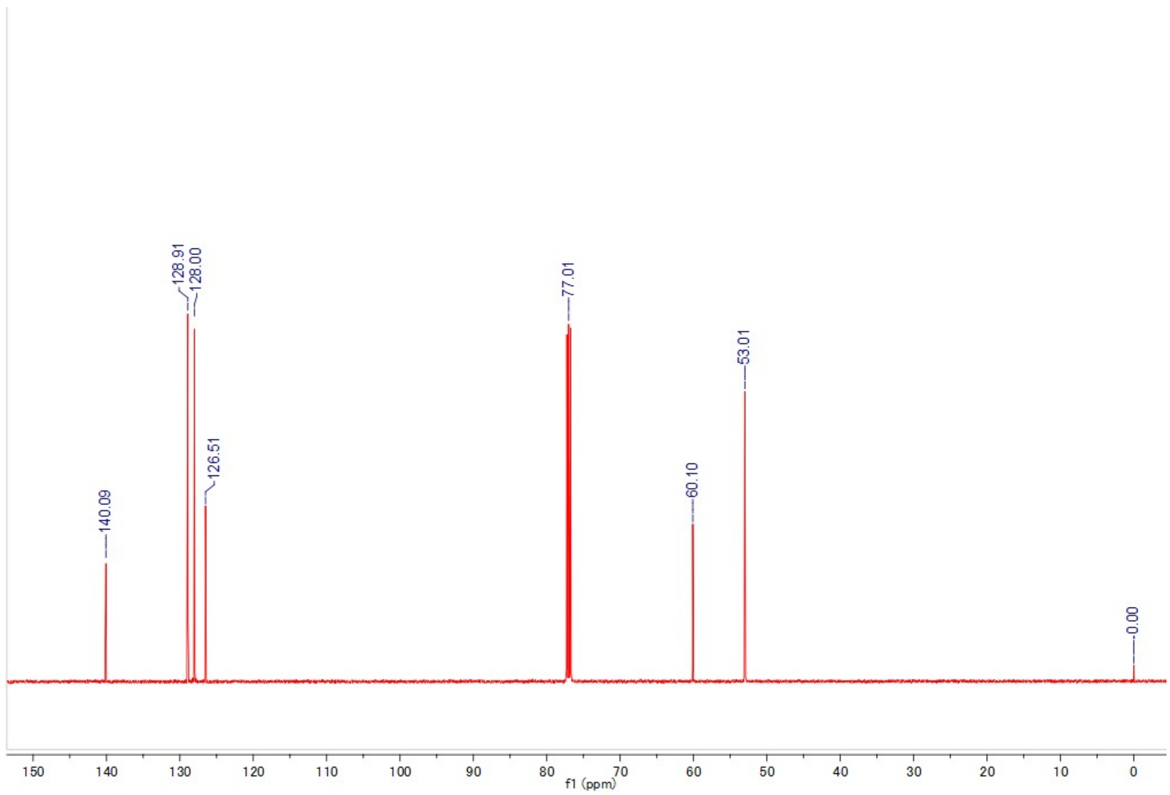

Fig. S4. ^{13}C NMR spectrum of (bn_4cyclen)

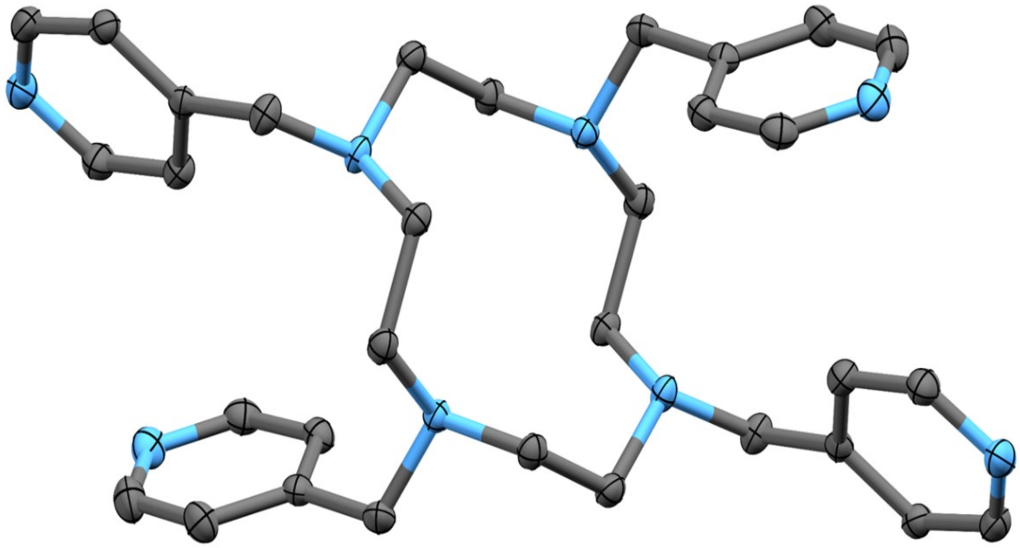

Fig. S5. ORTEP diagram of (pic)$_4$cyclen with thermal ellipsoids drawn at the 50% probability. Hydrogen atoms are omitted for clarity. Blue, N; gray, C.

Table S1. Crystal data for $(pic)_4$cyclen.

Radiation type, wavelength	Mo Kα, 0.71073
Formula	$C_{32}H_{40}N_8$
Formula weight	536.72
Crystal system	Triclinic
Space group	*P*–1
a (Å)	9.328(6)
b (Å)	9.338(5)
c (Å)	10.156(6)
α (deg)	95.874(3)
β (deg)	116.949(5)
γ (deg)	108.364(5)
V (Å³)	716.3(7)
Z	1
T (K)	93
d (g/cm³)	1.244
μ (mm^{-1})	0.077
R_1, wR_2 [$I > 2\sigma(I)$]	0.0463
R_1, wR_2 [all data]	0.1605
R_{int}	0.0290
F(000)	288
GOF	1.046

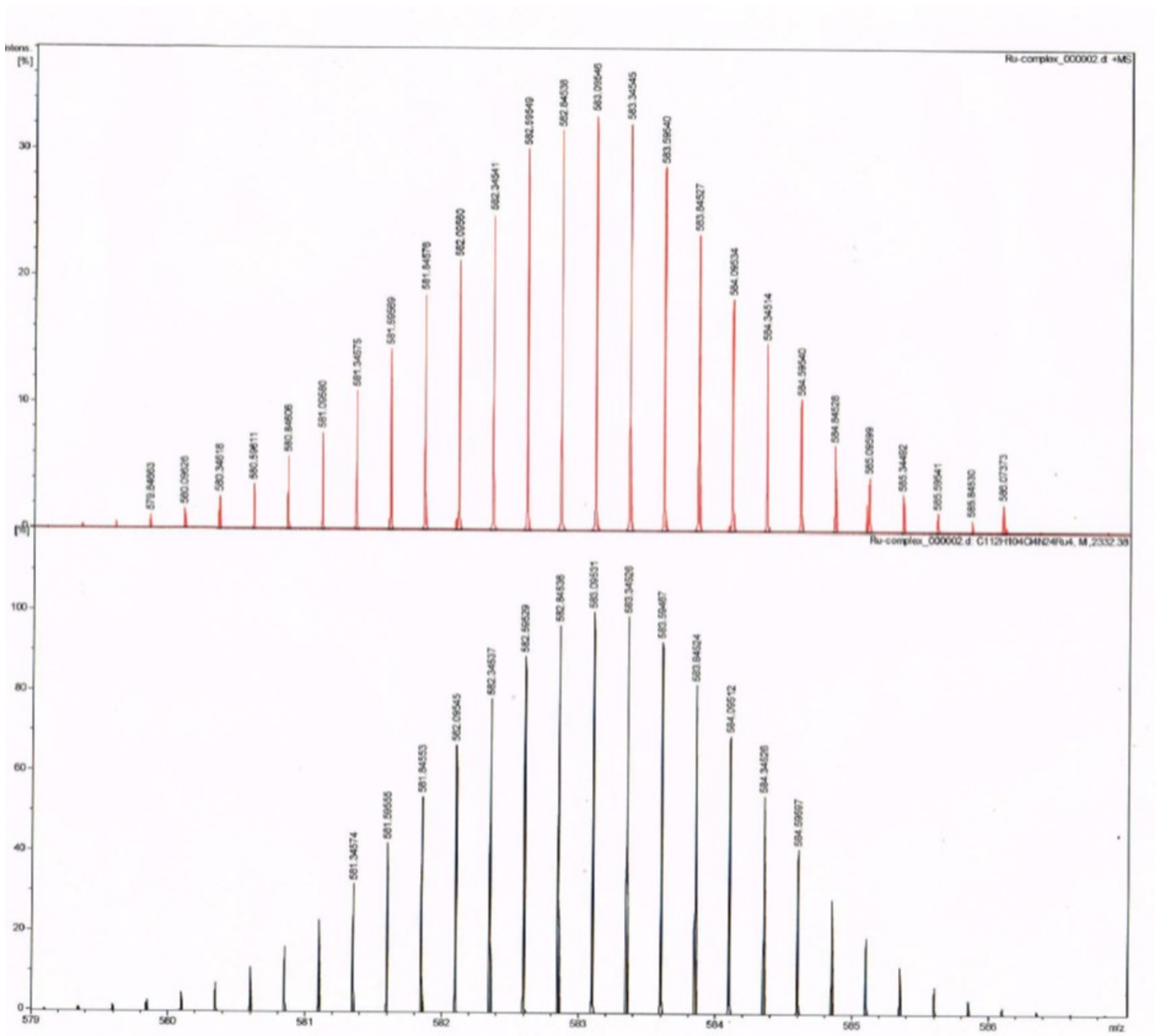

Fig. S6. ESI-Mass of $[([Ru]pic)_4cyclen]^{4+}$

Table S2. Crystal data for $[bn_4cyclenNiCl]Cl$.

Radiation type, wavelength (nm)	Mo Kα, 0.71073
Formula	$C_{36}H_{44}N_4NiCl_2$
Formula weight	662.36
Crystal system	Orthorhombic
Space group	$Ccm2_1$
a (Å)	7.7774(8)
b (Å)	25.294(3)
c (Å)	16.4763(17)
α (deg)	90
β (deg)	90
γ (deg)	90
V (Å^3)	3241.3(6)
Z	4
T (K)	298(2)
d (g/cm^3)	1.357
μ (mm^{-1})	0.795
R_1, wR_2 [$I > 2\sigma(I)$]	0.0530, 0.1327
R_1, wR_2 [all data]	0.0714, 0.1428
$F(000)$	1400
GOF	0.998

Table S3: Comparison of the coordination geometry of the Ni ion in $[bn_4cyclenNiCl]Cl$ to ideal geometries by using Shape 2.1.[1] A smaller value indicates better agreement.

Pentagon	Vacant octahedron	Trigonal bipyramid	Spherical square pyramid	Johnson trigonal bipyramid J12
D5h	C4v	D3h	C4v	D3h

33.267	2.854	5.429	0.181	8.959

The diffusion coefficient D calculation of [{([Ru]pic)$_4$cyclen}NiCl]$^{5+}$

The relationship between the cathodic peak current (i_p) and square root of the scan rate is given by the Randles-Sevcik equation for a homogeneous system.[2]

$$i_p = 0.4463 n_p F A [cat] (n_p F v D / RT)^{1/2} \qquad \text{Eq. S1}$$

where i_p is peak current (A), n_p is the number of electron(s) involved in the redox system (1 for $Ni^{II/I}$ redox process), F is the Faraday constant (96500 C·mol^{-1}), A is the surface area of working electrode (0.071 cm^2), $[cat]$ is catalysts concentration (mol·cm^{-3}), v is the scan rate (V·s^{-1}), R is the

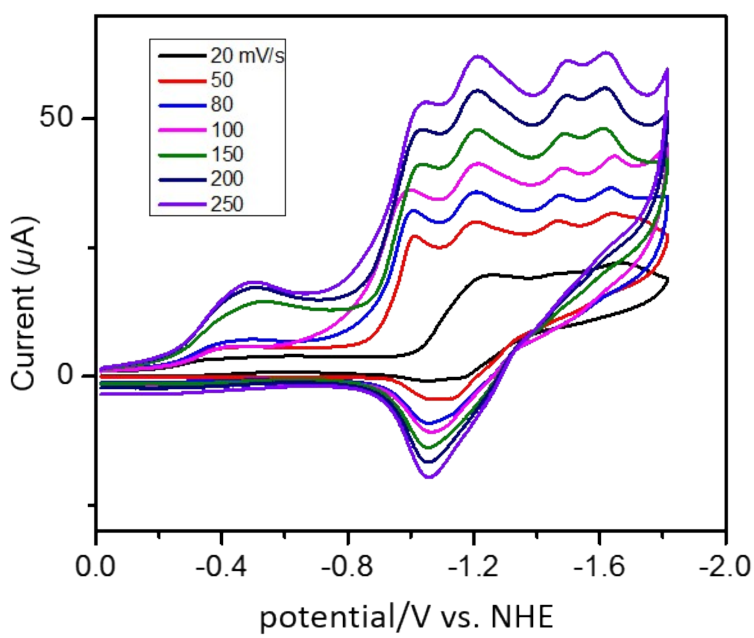

Fig. S7. Cyclic voltammograms of [{([Ru]pic)$_4$cyclen}NiCl]$^{5+}$ in CH_3CN containing 0.1 M $TBAPF_6$ at different scan rates. The $Ni^{II/I}$ couple was used as the cathodic peak current.

universal gas constant (8.31 J·K–1·mol–1), and T is the temperature (298 K). The diffusion coefficient D is calculated from the slop of i_p vs. $v^{1/2}$ plot.

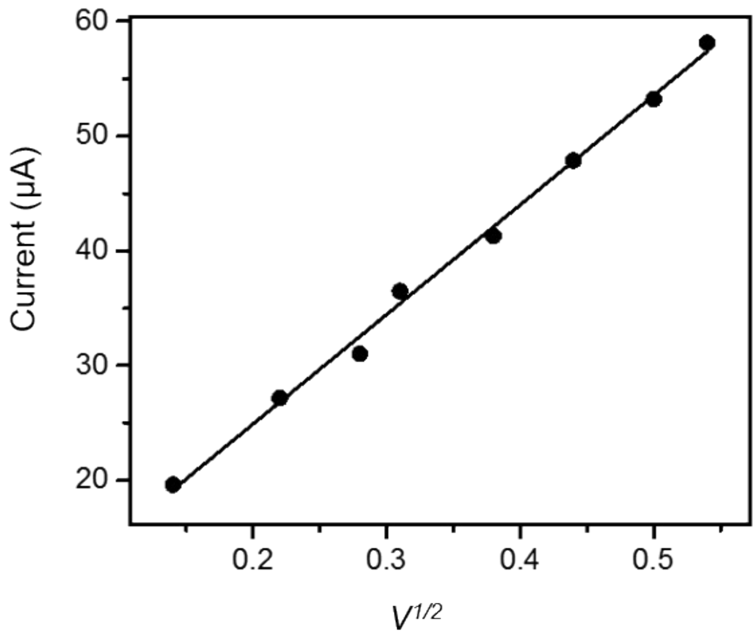

Fig. S8. Plot of i_p vs. $v^{1/2}$ for $[\{([Ru]pic)_4cyclen\}NiCl]^{5+}$, data collected from Figure 7. Peak current consider for $Ni^{II/I}$ reduction couples at corresponding scan rate. The current showing a linear dependence on scan rate, indicating that the reduction of for $[\{([Ru]pic)_4cyclen\}NiCl]^{5+}$ is a diffusion-controlled process.

The diffusion coefficient for for $[\{([Ru]pic)_4cyclen\}NiCl]^{5+}$ calculated using Eq. S1 to be 1.95×10^{-5} $cm^2·s^{-1}$.

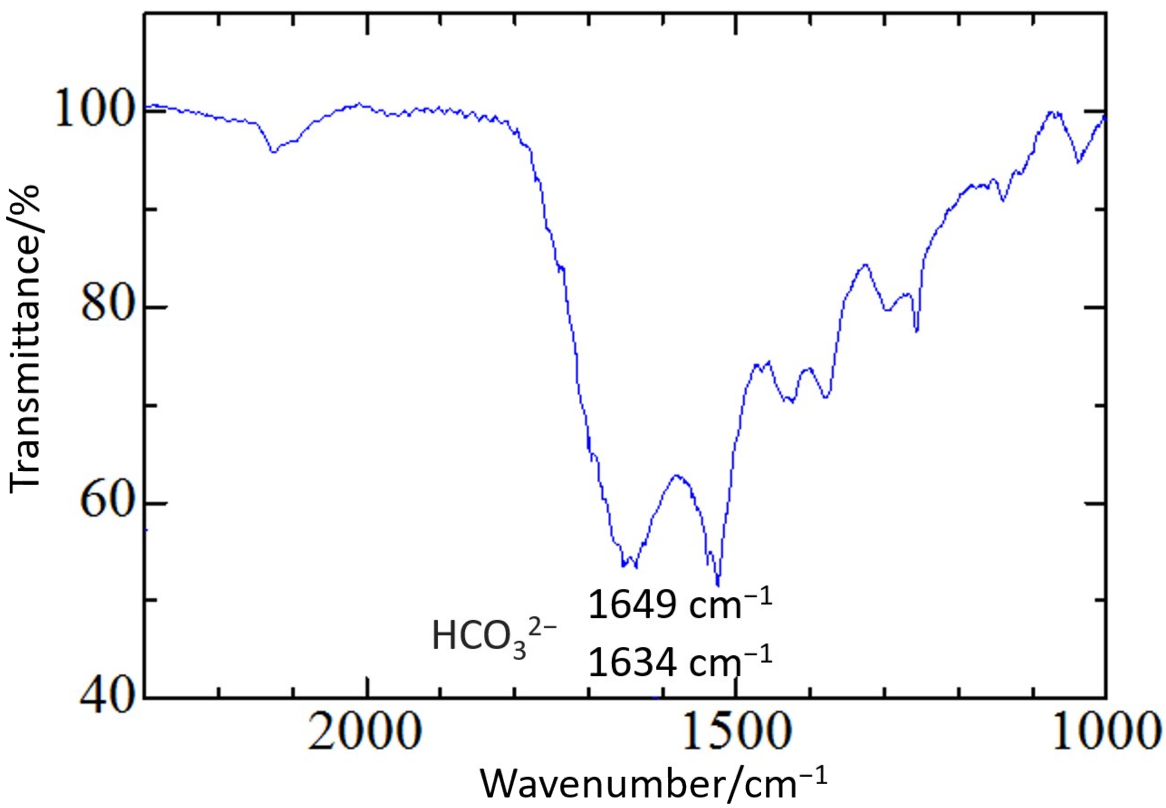

Fig. S9: IR spectroscopy of the solid collected after bulk electrolysis in dry CH_3CN.

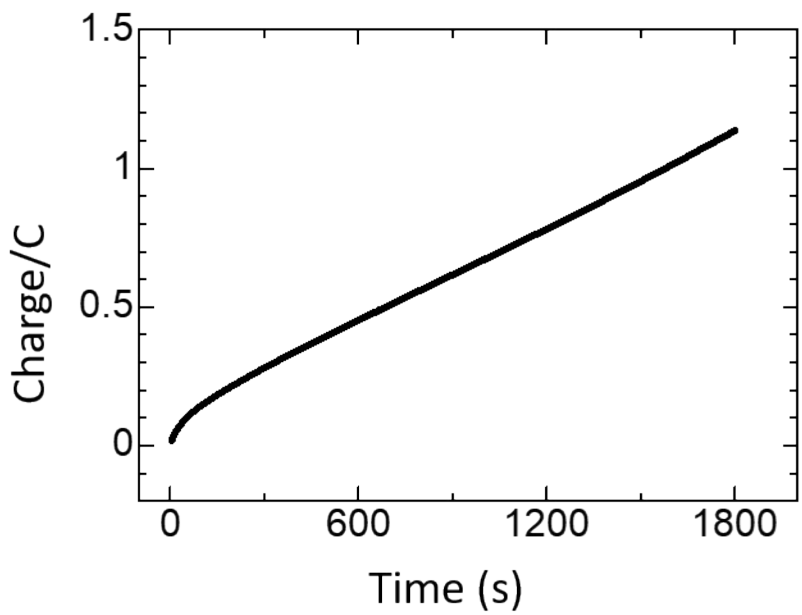

Fig. S10: CPE experiment trace for $[\{([Ru]pic)_4cyclen\}NiCl]^{5+}$

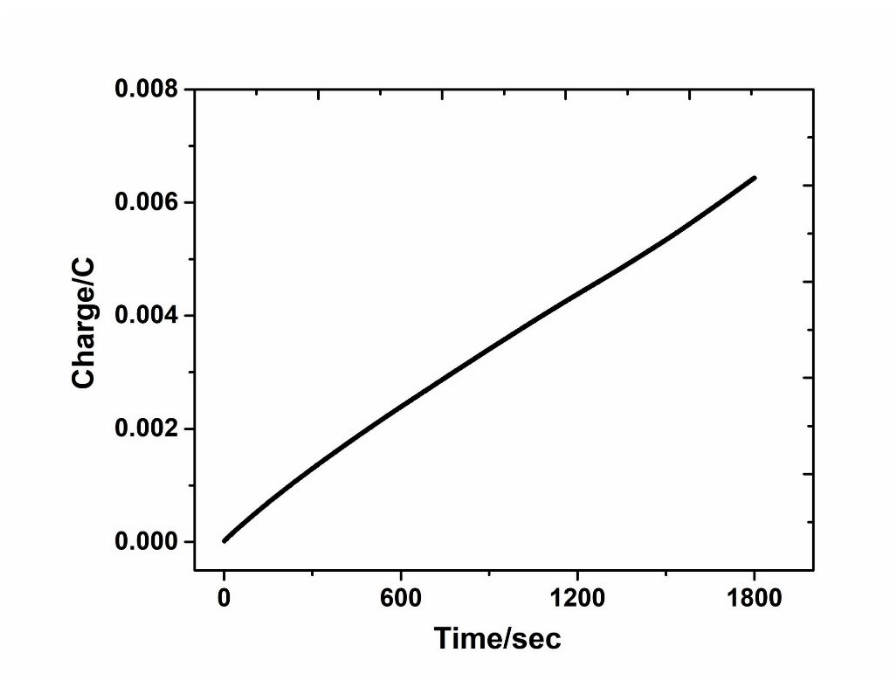

Fig. S11: CPE experiment trace for $[bn_4cyclenNiCl]Cl$

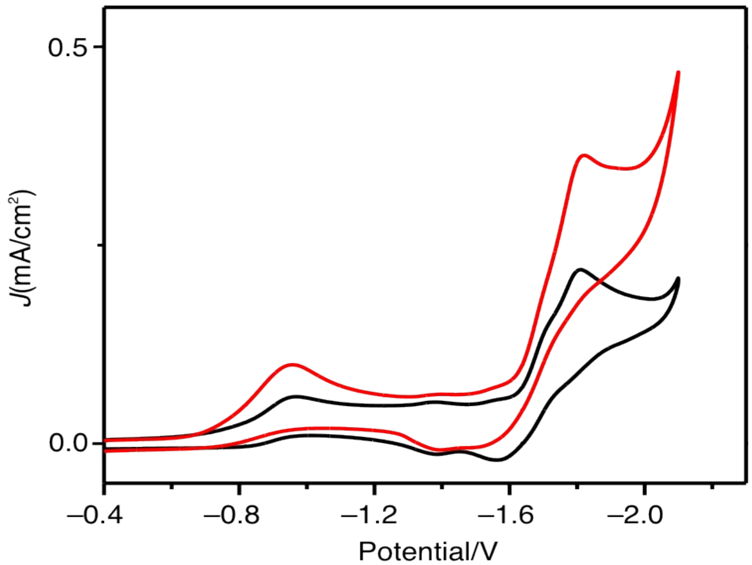

Fig. S12. Cyclic voltammogram of $[Ru(bpy)_2Cl]^+$ ([Ru]) vs. Ag wire under a N_2 atmosphere (black) and a CO_2 atmosphere (red). Although a small increase in the current was observed, it was small.

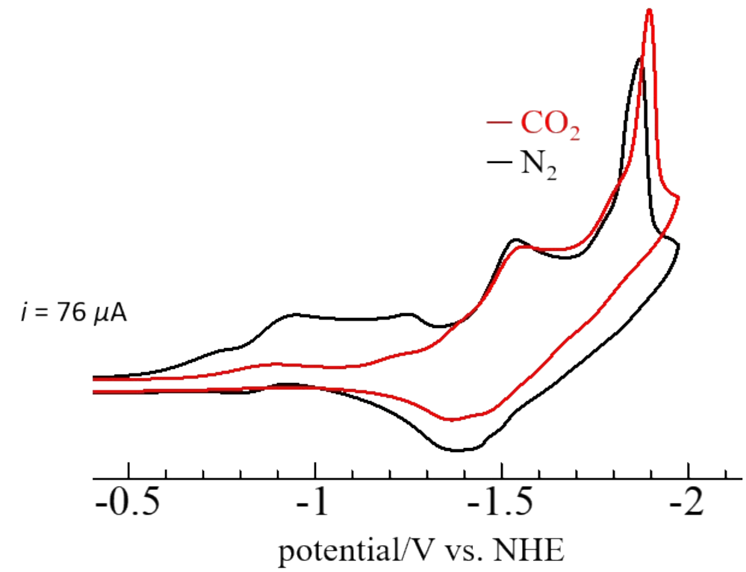

Fig. S13. Cyclic voltammetry of 1:4 [bn$_4$cyclenNiCl]Cl and Ru(bpy)$_2$Cl$_2$ under N_2 (black) and CO_2 (red) in 95:5 (v/v) CH_3CN/H_2O.

Table S4: Comparison of CO_2 reduction electrocatalysts

Entry	Catalyst	Major product	FE (%)	TOF(s^{-1})	η (V)	Ref.
1	$[\{([Ru]pic)_4cyclen\}NiCl]^{5+}$	CO	80	708	0.88	In this work
2	$[\{([Ru]pic)_4cyclen\}NiCl]^{5+}$	CO	84	178	0.53	In this work
3	$[bn_4cyclenNiCl]Cl$	CO	77	8	0.73	In this work
4	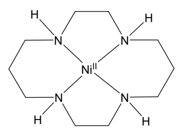	CO	84	130	0.55	3
5	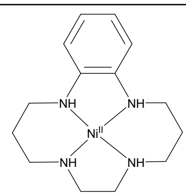	CO	88	100	0.59	3
6	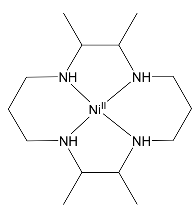	CO	88	100	0.55	3
7	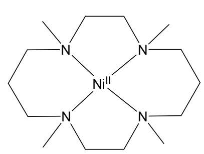	CO	90	90	0.88	4
8	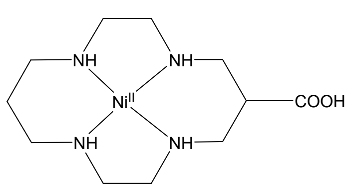	CO	86	190	0.65	5

Experimental TOF calculation

The experimental TOF was calculating based on, the total amount of CO generated during control potential electrolysis experiments divided by the total amount of catalyst in solution for electrolysis and then divided by time of control potential electrolysis. The equation given below.

$$TOF = \frac{\frac{n[CO]}{n[cat]}}{t} \qquad \text{Eq. S2}$$

Where, n[CO] is the total number of mole CO generate during electrolysis (from GC-MS measurement), n[cat] is the number of moles of catalysts in solution for using for electrolysis and t is the electrolysis time in seconds.

The experimental TOF from bulk electrolysis for $[\{([Ru]pic)_4cyclen\}NiCl]^{5+}$ and $[bn_4cyclenNiCl]Cl$ were calculated to be 2.64 s^{-1} and 0.09 s^{-1} in 5% H_2O/CH_3CN system, respectively.

References

1. S. Alvarez, P. Alemany, D. Casanova, J. Cirera, M. Llunell and D. Avnir, *Coord. Chem. Rev.* 2005, **249**, 1693–1708.
2. W. Nie and C. C. L. McCrory, *Chem. Commun*. 2018, **54**, 1579–1582
3. J. Schneider, H. Jia, K. Kobiro, D. E. Cabelli, J. T. Muckerman and E. Fujita, *Energy Environ. Sci*., 2012, **5**, 9502–9510.
4. J. D. Froehlich and C.P. Kubiak, *Inorg. Chem*., 2012, **51**, 3932–3934.
5. G. Neri, I. M. Aldous, J. J. Walsh, L. J. Hardwick and A. J. Cowan, *Chem. Sci*. 2016, **7**, 1521–1526.